

# Mechanical Properties of Double-Layer and Graded Composite Coatings of YSZ Obtained by Atmospheric Plasma Spraying

**Author names:** Pablo Carpio<sup>1,2</sup>, Emilio Rayón<sup>1</sup>, María Dolores Salvador<sup>1</sup>, Luca Lusvarghi<sup>3</sup>, Enrique Sánchez<sup>2</sup>

## **Affiliation:**

<sup>1</sup>Instituto de Tecnología de Materiales (ITM), Universitat Politècnica de València. Camino de Vera sn/, 46022 Valencia, Spain

<sup>2</sup>Instituto de Tecnología Cerámica (ITC), Universitat Jaume I. Campus Universitario Riu Sec, Av. Sos Baynat s/n, 12006 Castellón, Spain

<sup>3</sup>Dipartimento di Ingegneria “Enzo Ferrari”, Univeristà degli Studi di Modena e Reggio Emilia. Via Univeristà 4, 41121 Modena, Italy

**Corresponding author:** Pablo Carpio

**Email:** [pabcarco@upv.es](mailto:pabcarco@upv.es)

## **Abstract**

Double-layer and graded composite coatings of yttria stabilised zirconia (YSZ) were sprayed on metallic substrates by atmospheric plasma spray (APS). The coatings architecture was built up by combining two different feedstocks: one micro- and one nano-structured. Microstructural features and mechanical properties (hardness and elastic modulus) of the coatings were determined by FE-SEM microscopy and nanoindentation technique respectively. Additional adherence and scratch tests were carried out in order to assess the failure mechanisms occurring between the layers comprising the composites.

Microstructural inspection of the coatings confirms the two-zones microstructure. This bi-modal microstructure which is exclusive of the layer obtained from the nano-structured feedstock negatively affects the mechanical properties of the whole composite. Nanoindentation tests suitably reproduce the evolution of mechanical properties through coatings thickness on the basis of the position and/or amount of nano-structured feedstock used in the depositing layer.

Adhesion and scratch tests show the negative effect on the coating adhesion of layer obtained from the nano-structured feedstock when this layer is deposited on the bond coat. Thus the poor integrity of this layer results in lower normal stresses required to delaminate the coating in the adhesion test as well as minor critical load registered by using the scratch test.

**Keywords:** Plasma spraying; thermal barrier coatings; multilayer coatings; functionally graded materials; adherence; nanoindentation

## **1. Introduction**

The most used material of thermal barrier coatings (TBCs) is currently yttria-stabilised zirconia (YSZ) due to its low thermal conductivity, relatively high coefficient of thermal expansion, phase stability and high corrosion resistance [1]. With regard to processing, atmospheric plasma spraying (APS) is one of the most common techniques to produce these coatings due to its good balance between coating performance and low cost [2]. However in the last years the need of increasing the operational temperature of gas turbines has fueled an intense research activity to develop coatings systems with enhanced thermal insulation, in particular low thermal conductivity [3,4]. In this sense, in previous research it has been demonstrated that using fine (nano- or submicron-structured) instead of coarse (microstructured) powder as plasma feedstock gives rise to coatings with lower thermal conductivity. This is because these coatings are made up of a melted matrix with a significant presence of unmelted or partially melted areas containing porous nano- or submicron-sized zones which are mostly responsible for a further reduction of thermal conductivity as reported elsewhere [5,6]. Nevertheless, these fine-structured zones forming the coatings are more prone to sintering effect which results in coatings more sensitive to the effect of treatment temperature during the potential use of the TBC [5-7].

This need to comply with the advanced TBC coatings requirements has also led to look for new TBC materials, the development of new coating architecture for the existing materials or a combination of both approaches. Thus new materials, stable at higher temperatures and with lower thermal conductivity than YSZ, multilayer systems with different functions or graded

structures changing the composition from interface with bond coat to the surface are now under intense research activity [8-12]. The present ~~research~~ study is focused on controlling the coating architecture by tailoring its microstructure, keeping zirconia as coating material.

The above considerations suggested the interest of exploring for the first time the possibility of combining the properties/performance of conventional (microstructured) and nano-structured layers in designing new types of YSZ-based TBCs, using their respective benefits. This idea was put in practice in a research which has been previously reported [13]. As set out in this first paper, it was considered that these composite coatings might be obtained by using two approaches: a double-layer (multilayer) assembly of micro- and nano-structured layers and a graded composite, in which the composition of the micro- and/or nano-structured feedstock-containing layers could be gradually changed in a graded architecture. In this first part of the research, the microstructure and hardness of the resulting composite coatings were investigated.

Findings in this first part showed that the multilayer coating microstructure exhibited two clearly distinct areas, defined by the amount of partially melted areas (PM areas), which were in turn directly related to the layer deposited using the nano-structured feedstock. The PM areas were thus exclusively concentrated in the layer obtained from the nano-structured feedstock. This caused a marked change in hardness across the coating thickness, as the layers in these composites largely preserved the hardness of the corresponding reference single-layer coating. On contrary in the graded coatings, the amount and size of the PM areas gradually varied (increasing or decreasing) from the bond coat interface to the top layer, paralleling the variation in nano-structured

feedstock content in the deposited mixture. There was no distinct interface between any two adjacent layers, and a gradual change in hardness was observed.

Due to the interesting findings obtained in this first part of the research by designing different nano- and microstructured composite coatings a further research was planned with the aim at deepening on the relationship between the microstructure and mechanical properties of these new composite coatings. Bearing this aspect in mind, nanoindentation mechanical characterisation was addressed. Nanoindentation technique has been successfully used for characterisation of mechanical properties of plasma spray coatings because this technique allows to easily distinguish the melted and partially melted areas in the coatings and therefore to correlate these areas with mechanical properties by determining elastic modulus and/or hardness of different points throughout the coating cross-section [14,15]. Thus ~~first part of the research~~ previous works have shown that elastic modulus and hardness in titania or YSZ coatings can widely vary on the basis of the amount of partially melted areas present in the coatings while the porosity and sintering degree of these partially melted areas can also play a role [5].

As a consequence of the above the objective of this paper is to evaluate the mechanical behavior of multilayer and functionally-graded coatings. First, two double-layer coatings were obtained, depositing the micro- on the nano-structured feedstock in the first coating and performing the deposition in the opposite order in the second one. Secondly, two graded coatings were obtained, progressively depositing increasing or decreasing amounts of micro- or nano-structured feedstock in mixtures of both feedstocks. In particular, the

paper aims to determine the mechanical properties (elastic modulus and hardness) throughout the coatings by nanoindentation as well as to try to relate these mechanical properties with the nano- and micro-structure of the coatings. Besides, adhesion and scratch tests were also carried out in order to assess the failure mechanisms occurring during mechanical testing of coatings.

## **2. Experimental**

### **2.1. Design and preparation of double-layer and graded composite coatings**

The design of the two types of composite coatings (double-layer and graded) was based on two commercial feedstock powders of  $Y_2O_3$ -stabilised  $ZrO_2$  (YSZ): one used for obtaining conventional (microstructured) coatings (Metco 204NS, Oerlikon Metco, Germany) and the other used to deposit nanostructured layers (Nanox<sup>TM</sup> S4007, Inframat Advanced Materials, USA). The weight ratio of constituent oxides ( $Y_2O_3:ZrO_2$ ) of both powders were very similar: 8:92 and 7:93 for the microstructured and the nano-structured powders respectively. An exhaustive characterisation of both powders can be found elsewhere [16,17]. As previously reported both powders consisted of spherical granulates of agglomerated particles, whose average size was about 400–800 nm in the conventional powder and 200 nm in the nano-structured powder. Their morphology suggests that both powders were obtained by a spray-drying process. In addition, the conventional powder underwent a thermal treatment to partially sinter their agglomerates. This type of partially sintered granulate feedstock is generally known as HOSP (hollow spherical powder) [16].

The YSZ layers of the two feedstocks were deposited onto stainless steel (AISI 304) substrates by an atmospheric plasma spray (APS) system. The system consisted of a gun (F4-MB, Sulzer Metco, Germany) operated by an industrial robot (IRB 1400, ABB, Switzerland). Before spraying, the substrate was grit-blasted with corundum at a pressure of 4.2 bar and cleaned with ethanol to remove any remaining dust or grease from the surface. A bond coat (AMDRY 997, Sulzer-Oerlikon, Germany) was used to enhance the adhesion between the substrate and the ceramic layers. Bond coat composition was Ni-23Co-20Cr-9Al-4.2Ta-0.6Y (weight fraction, %). Deposition was performed using argon and hydrogen as plasma-forming gases.

Two independent feed systems (one for each powder), with their respective circuits, were used to obtain the multilayer and the graded coatings. The two powders were thus injected into the plasma plume via two different nozzles arranged radially around the torch. To assure adequate powder flow through each feed system, 3 slpm (standard litre per minute) of argon flow was used. A flow diagram describing this process as well as the resulting composite coatings is shown in figure 1. More information about the spraying parameters as well as the deposition process can be consulted in [13].

As it can be seen in figure 1 two double-layer composite coatings were designed: the M1 coating which was obtained by first depositing the conventional and then the nano-structured feedstock and the M2 coating which was obtained by depositing the feedstocks in the opposite order. Besides two graded composite coatings were designed: the G1 coating in which the bottom layer consisted of a 100% conventional powder deposition and the top layer a 100% nano-structured powder deposition and the G2 coating in which the

opposite order was used. Five layers were prepared for each graded coating, using the following composition for each feedstock: 100%, 75%, 50%, 25%, and 0%. The total thickness of each composite coating (both M and G) was about 150  $\mu\text{m}$ .

## **2.2. Coating characterisation**

A field-emission scanning electron microscope JEOL 7001F, Jeol Lt., Japan) and an optical microscope (Eclipse LV100, Nikon, Japan) ~~was~~ were used to analyse coating microstructure on the polished cross-section areas. Optical microscopy images were also employed to help the nanoindentation findings interpretation. The nanoindentation analysis was performed by a G-200 nanoindenter (Agilent Technologies, USA) using a diamond Berkovich tip whose function area was carefully calibrated on a silica material at low depths. The stiffness was calculated by a Continuous Stiffness Measurement mode set at 2 nm harmonic oscillation amplitude and at 45 Hz oscillation frequency. Three arrays of 20 indentations at a 400 nm maximum constant depth were performed on polished cross-section of the coatings. The location of the first test was guided by an optical microscope and the subsequent indentations were programmed to be distanced between them by 8  $\mu\text{m}$ , 20 times the maximum depth which is the minimum distance to avoid the interference among indentations. Subsequent hardness and elastic modulus calculation was considered between 100 and 200 nm as reported elsewhere [18].

A Revetest scratch testing instrument (CSM Instruments, Switzerland) was used to study the failure mechanism of sprayed layers. Several scratches were tested on randomly chosen positions of double-layer M1 and M2 samples



surfaces using a 200  $\mu\text{m}$  diameter Rockwell diamond stylus. A progressive load from 1 to 200N at 5mm/min speed was applied to scratch a track of 10 mm length. The load and reached depth were recorded during the test. The grooves were observed and recorded by an optical microscope with a video camera installed in the same scratch tester.

Finally an automatic Adhesion Tester (PosiTest AT-100, DeFelsko, USA) was used to measure the substrate/bond coat/top coat adhesion strength. The test procedure is simple; several specimens made as metallic discs (dolly) are glued on the surface of coatings by special epoxy glue (maximum shear strength 25.5 MPa, Araldite serie 2000, Hunstman, USA). An electronically controlled hydraulic pump automatically applies smooth and continuous pull-off pressure at a userspecified rate until the adherence falls and the coating is peeled-off. At this moment, the glued coating beyond dolly is released (peeled-off) and subsequent observation serves to corroborate how the failure was produced; that is, by adhesive failure between substrate and bond coat, between bond coat and the deposited coating or by cohesive breakage inside the same coating. Furthermore, the ultimate force is registered by the instrument and the adhesion strength is then calculated. The manufacturer ensures a pressure system calibrated with certified  $\pm 1\%$  accuracy. For this study, four 10mm diameter dollies were glued on each coating assuring that enough distance between them was kept. The tensile test was subsequently experimented recording the maximum strength reached.

### **3. Results and discussion**

#### **3.1 Microstructure dependence of mechanical properties**

The microstructure of the present coatings is the result of combining the typical microstructures obtained from conventional HOSP and nano-structured spray-dried feedstocks. In previous works, it has been reported that coatings from HOSP (microstructured) powders displayed the conventional APS microstructure formed by fully melted (FM) splats with the presence of microstructural features (voids and cracks). However, coatings from porous spray-dried (nano-structured) powders display a bimodal structure with partially melted (PM) areas rounded by a fully melted (FM) material. The reason of the apparition of these partially melted areas is because the agglomerates are bigger and more porous for the nano-structured powder compared to the HOSP, therefore the heat transmission up to the agglomerate center inside the plasma plume is lower [16,17].

By changing the deposition sequence of the feedstocks (double-layer composites) as well as the composition of the feedstock mixture (graded composites) several coatings with diverse PM/FM ratios were obtained. As a summary, figure 2 describes the microstructure of the four composite coatings obtained by SEM microscopy. A first inspection of these micrographs reveals the deposited ceramic coating (top coat) onto the bond coat showing the typical splat-like microstructure and PM and FM zones (marked PM and FM in the figure). As also observed in this figure the double-layer coatings microstructure (M1 and M2) exhibits two clearly distinct areas, defined by the amount of partially melted areas (PM areas), which were in turn directly related to the layer deposited using the nano-structured feedstock. The PM areas were thus exclusively concentrated in the layer obtained from the nano-structured feedstock. Similar situation was observed for the graded composites (figures 2c

and 2d) although in this case, the microstructural changes between top and bottom part of the coating were gradual. Nonetheless, regardless the type of coating the PM layers never appeared as a continuous layer in contrast to the melted layer, it can be probably because fully melted powders can easily flatten when impacting on the substrate while partially melted powders are still solid inside so that they cannot properly flatten.

With the aim to find a relation between microstructure and mechanical properties nanoindentation test was carried out on the cross sections of the four coatings (M1, M2, G1 and G2) as set out above. Figure 3 (from a to d) collects the findings of average elastic modulus and hardness obtained from the nanoindentations performed across the cross-sections of the different composite coatings. For the sake of better understanding the nanoindentations profile the background of the elastic modulus plot of any of the coatings has been represented by the actual images of the composite coatings. The high dispersion of values found in these curves is due to the heterogeneous topography of the melted and partially melted areas provoked by the polishing procedure and to the fact that three arrays performed on different places of the coating were averaged.

The nanoindentation measurements confirmed that mechanical properties changed across the thickness in the same way that coating microstructure changed, as it was reported in [13]. High values of PM areas inside coatings diminishes the resultant hardness and elastic modulus (see particularly the right end of the hardness plot of figure 43a). Thus steady values of 15GPa and 200GPa for hardness and elastic modulus, respectively, were determined for the layers obtained from the microstructured feedstock in coatings M1 and M2

(figures 43a and 43b) while these values diminished gradually down to 2.5GPa and 25GPa for the layers obtained from the nano-structured feedstock in these same coatings. Therefore, the worst values of nano-mechanical properties measured on layers obtained from the nano-structured feedstock indicate that the heterogeneous microstructure made up of pores and above all partially melted areas associated with these layers prevails over the hardening effect expected from a nano-structured ceramic material [19]. The role of porosity and, particularly the amount of partially melted or unmelted areas on the mechanical properties of APS coatings obtained from nano-structured feedstocks has been previously reported for YSZ and other oxide coatings such as alumina and titania [17,20]. In fact, in these papers nanoindentation technique was explicitly recommended to identify the partially melted areas of coatings obtained from nano-structured feedstock due to the low values of mechanical properties associated with these areas.

On the other hand, as observed in figure 23, the double-layer coatings (samples M1 and M2) clearly show a drastic change in their mechanical properties, as it is also observed in the microstructure, which as reported reproduces the change from the layer obtained from the microstructured feedstock to the layer obtained from the nano-structured one [13]. This means that where the layer from the nano-structured feedstock is present, the steady values of mechanical properties are much lower because the PM/FM area ratio is higher. This abrupt change is particularly observable when the porous layer, i.e. the layer obtained from the nano-structured feedstock lies on the bond coat. This finding confirms the need of depositing the most dense and tough layer on the bond coat when a multilayer composite coating is designed since the bond coat-top coat interface

is considered as a high stress zone [10,12]. On contrary, the impairing of mechanical properties associated with the layers obtained from the nano-structured feedstock is, as expected, more gradual in the composite coatings, in particular for the G1 coating in which 100% nano-structured feedstock was deposited on the top of the coating, i.e far away from the bond coat. In fact hardness of the G2 coating is also strongly affected by the weak nano-structured layer placed on the bond coat.

### **3.2 Coating failure mechanism analysis by means of adherence and scratch testing**

The way in which mechanical properties (elastic modulus and hardness) are distributed along the two types of composite coatings will certainly impact on failure mechanism of the coatings. For this reason the analysis of the failure mechanism of the coatings was assessed by means of two mechanical tests: adhesion strength and scratch resistance.

Firstly, the coatings were tested using a normalised adhesion test by stressing a glued dolly on surface coating assuring sufficient pull-load so as to peel-off the layer. The figure 4 shows the captured pictures of the material removed from the coating (dolly side) as well as the provoked crater in the coating (coating side). The images a) and c) corresponds to M1 and G1 coatings which contained the layer deposited from the microstructured feedstock next to the bond coat. On contrary the b) and d) images represent M2 and G2 coatings which had the layer obtained from the nano-structured feedstock on the bond coat.

As it can be easily seen the a) and c) craters display similar aspect since these craters manage to uncover large areas of bond-coat which are visible as grey metallic surfaces. In the case of the coating M1 the uncovered surface is even higher than that of the G1 sample. This feature indicates a possible delamination failure mechanism between top and bond coats. To confirm this hypothesis, a cross-section view of some samples were observed by optical microscopy, as shown by the representative acquired image in figure 5 (coating M1). Thus, as observed in this figure, the top coat delaminates from the bond coat which keeps a good adhesion on substrate. These findings confirm the good influence on the whole coating of the layer deposited from the microstructured feedstock when it lies on the bond coat. Thus as observed in figure 23 higher and more homogeneous values of mechanical properties are obtained through the coatings thickness in coating M1 when compared with coating M2 in which the layer obtained from the nano-structured coating was sprayed on the bond coat. In addition as figure 23 reveals the variation of mechanical properties in coating M1 is much more gradual than that of the coating M2 giving rise to an enhanced integrity of the entire double-layer coating.

Figure 4 also shows that samples b) and d), which correspond to composite coatings prepared from nano-structured feedstock directly deposited on the bond coat, underwent lower material removal than that of the a) and c) samples as revealed by the lower amount of uncovered areas of bond-coat. Thus the cross-section view in figure 5 (coating M2) indicates an adhesive failure in the layer of the top coat obtained from the nano-structured feedstock probably as a consequence of the boundary grain failure inside the partially melted areas which are very abundant in this mentioned layer. The registered adhesion

strengths of the four coatings are summarised in table 1. These values fall within the same range of the adhesion strengths of TBC measured with the same tester published in previous works [21]. As observed, coatings in which the layer obtained from the microstructured feedstock lies on the bond coat give rise to higher adhesion strengths, in particular the M1 coating. On contrary the lower adhesion strength obtained for coating M2 in which the layer closer to the bond coat was deposited from the nano-structured feedstock corroborates the hypotheses of the mechanism explained above. It is also noteworthy highlighting the differences between Ms and Gs composites. The graded composites display a gradual variation in microstructure (partially melted areas) as well as in coating cohesion between layers resulting in a much more homogenous behaviour of the overall top coat in terms of adhesion strength when compared with top coats of M1 and M2 composites. In applications where a high erosion or corrosion resistance is necessary, depositing the conventional (microstructured) layer as top coat could be an interesting approach because lower porosity on the top layer can enhance the wear resistance or impede the glass corrosion of the coatings [20,22]. In these cases, graded composite coating (G2) optimises all these requirements representing a clear improvement with respect to the multilayer coating (M2).

With regard to scratch testing this determination represents a powerful hardness dynamical technique that provides a valuable comparative data about the load required to provoke failure of a given sample when a stylus tip slides on a surface under a programmed load [23,24]. This load of failure is also called the critical load. In this research only the double-layer composites M1 and M2 were tested due to the greater differences observed in microstructure and

mechanical behaviour of these two coatings when compared with the corresponding coatings of the graded composite (G1 and G2). Figure 6 shows the pictures of the scratch grooves on coatings produced by the scratch test and the corresponding penetration curves of the tip. Penetration curves were registered during the scratch test (under the scratch load) and subsequently again registered after the test by scanning the reached depth groove under very low loads.

With regard to the scratch grooves it should be first explained that the bond coat is revealed as a metallic-looking track surrounded by a black region which represents the coating material ploughed by the scratch tip. However a clear distinction between the two coatings with regard to the point (scratch length) at which the black region shows up is not easy. Thus the metallic aspect of the groove seems to be developed at scratch length >5 mm for the coating M1 and at earlier position <5 mm for coating M2. The appearance of the groove indicated a plastic and/or adhesive failure in both cases without observable cracks or other failure mechanism.

Much more quantitative assessment can be worked out by means of the penetration curves of these same two double-layer composite coatings as plotted in figure 6. Thus several behavior differences can be observed between the two samples which agree with the qualitative appreciation obtained from the scratch groove observation set out above. The curve of M1 coating (layer deposited from the microstructured feedstock on the bond coat) reveals that penetration curves follow a continuous and constant penetration rate till approximately 80 N (3.5 mm displacement) which is related with the tip penetration through the layer of the nano-structured feedstock. Over this load or



penetration the penetration rate slope is reduced which coincides with the stiffer layer obtained from the microstructured feedstock. A further change of penetration rate slope is observable when the tip penetrates into the bond coat. This fact starts to occur at approximately 6.5 mm displacement (~125 N load) which agrees with the observation of the metallic footprint in the scratch groove. A very different behaviour resulted when the layer obtained from the nanostructured feedstock was deposited immediately on the bond coat (coating M2) as revealed by figure 6. The penetration curve shows a lower critical load. It was detected at ~60N (~ 2.5 mm displacement) when penetration curve sharply falls until the surface of bond coat. It means nano-structured layer accelerates the tip penetration in this composite. This finding again agrees with the observation of the metallic footprint in the scratch groove. Another critical load was recorded at higher loads when the steel substrate is reached. The approximate depth of each layer is determined from the microstructure cross-section view. On comparing both figures it is evident that the cutting shear stresses provoked by the friction efforts lead to more severe damages at lower loads when the layer obtained from the nano-structured feedstock is deposited immediately on the bond coat.

Overall adhesion and scratch tests confirm the findings reported in the first part of this research. Thus the layer obtained from the nano-structured coatings which is characterised by low elastic modulus and hardness drastically affect to the bulk mechanical properties of the global composite (double-layer) coating. Moreover this such a weak layer negatively impacts on the adhesion of the composite coating on the bond coat. On contrary, the deposition of the layer obtained from the conventional feedstock on the bond coat gives rise to a much

better situation in terms of bulk mechanical properties as well as coating adhesion. In this case (coating M1) the effect of the weaker layer (from the nano-structured feedstock) deposited on the stiffer one (obtained from the conventional feedstock) hardly affect the adhesion and cohesion of the overall composite coatings while further benefits of this more porous and unmelted layer on the thermal cycling behaviour of the composite coating can be expected.

The findings presented in this research agree with recent publications by Sampath et al [10] on advanced multilayer TBC of YSZ. Thus these authors have proposed novel bilayer architectures in an effort to improve thermal cycling of the TBC. This bilayer approach is based on depositing a dense coating at regions prone to bond coat interface where delamination usually occurs while allowing for the rest of the coating to contain high porosity in order to obtain a low modulus layer. Variations in porosity were achieved by changing plasma spray conditions. Similar objective was addressed by Vassen et al in another reported work on porosity graded TBC composites which likewise were designed by modifying plasma spray conditions [12]. Unlike this reported research in this paper changes in mechanical properties of the constituents' layers of multilayer or graded composites have been obtained by modifying the characteristics of the feedstocks (micro- or nano-structured) which as set out throughout the research gave rise to very different amount of unmelted areas in the coatings finally resulting in substantial variations of mechanical properties.

Nevertheless further research is still necessary so as to demonstrate if the new designed composite coatings (bilayered or graded) based on micro- and nanostructured feedstocks are capable of enhancing durability and functional

performance of the TBC. In this sense, thermal fatigue resistance and molten glass attack are necessary tests to further evaluation of these coatings.

#### **4. Conclusions**

Two series of composite coatings of TBCs based on YSZ have been designed and characterised. These composite coatings were deposited from two different feedstocks: a microstructured HOSP powder and a nano-structured spray-dried agglomerated one. The first series of composites consisted of two double-layer coatings (double-layer composite) made up of one deposited layer of the microstructured feedstock and another layer of the nano-structured one. Layers obtained from each one of the feedstocks displayed the expected microstructure: on one hand a conventional APS layer from HOSP powders and on the other hand a bimodal layer with partially melted zones nano-structured spray-dried agglomerates. The second series of two composites was built up by gradually changing the composition of the deposited layer made up of mixtures of the two feedstocks (graded composite).

A deeper insight into mechanical properties (hardness and elastic modulus) has been addressed by nanoindentation technique as well as by the analysis of the mechanical failure of these two series of composites by measuring adhesion and scratch resistance.

Nanoindentation findings confirm an abrupt or gradual change in mechanical properties for the double-layer and graded composites respectively which depend on the amount of unmelted areas in the coatings provided by the deposited nano-structured feedstock. In the double-layer composite the

magnitude of the change is even more detrimental when the layer deposited from the nano-structured feedstock lies on the bond coat. This negative effect is confirmed by adhesion test. Thus delamination of the layer obtained from the nano-structured feedstock has been observed when this feedstock is deposited on the bond coat. This negative effect is even observable in the graded coatings. Finally scratch testing corroborates the weak point provided by the layer obtained from the nano-structured feedstock when is placed next to the bond coat since the collapse of the coating takes place at quite low penetration load. On contrary some benefits of depositing this feedstock on the top layer could be expected in relation with coating durability which should be investigated by further research.

### **Acknowledgments**

This work has been supported by the Spanish Ministry of Science and Innovation (project MAT2012-38364-C03) and co-funded by ERDF (European Regional Development Funds).

### **References**

- [1] Y.S. Tian, C.Z. Chen, D.Y. Wang, J.I. Quianmao, Recent Developments in Zirconia Thermal Barrier Coatings, *Surf. Rev. Lett.*, 2005, **12**, p 369-378
- [2] S. Sampath, U. Schulz, M.O. Jarligo, S. Kuroda, Processing Science of Advanced Thermal-Barrier Systems, *MRS Bull.*, 2012, **37**(10), p 903-910
- [3] D.R. Clarke, M. Oechsner, N.P. Padture, Thermal-Barrier Coatings for More Efficient Gas-Turbine Engines, *MRS Bull.*, 2012, **37**(10), p 891-898

- [4] A. Feuersein, J. Knapp, T. Taylor, A. Ashary, A. Bolcavage, N. Hitchman, Technical and Economical Aspects of Current Thermal Barrier Coating Systems for Gas Turbine Engines by Thermal Spray and EBPVD: A Review, *J. Therm. Spray Technol.*, 2008, **17**(2), p 199-213
- [5] R.S. Lima, B.R. Marple, Thermal Spray Coatings Engineered from Nanostructured Ceramic Agglomerated Powders for Structural, Thermal Barrier and Biomedical Applications: A review, *J. Therm. Spray Technol.*, 2007, **16**(1), p 40-63
- [6] P. Fauchais, G. Montavon, R.S Lima, B.R. Marple, Engineering a New Class of Thermal Spray Nano-based Microstructures from Agglomerated Nanostructured Particles, Suspensions and Solutions: an Invited Review, *J. Phys. D Appl. Phys.* 2011, **44**(9), 093001
- [7] P. Carpio, Q. Blochet, B. Pateyron, L. Pawlowski, M.D. Salvador, A. Borrell, E. Sánchez, Correlation of Thermal Conductivity of Suspension Plasma Sprayed Yttira Stabilized Zirconia Coatings with some Microstructural Effects, *Mater. Lett.*, 2013, **107**, p 370-373
- [8] R. Vassen, A. Stuke, D. Stöver, Recent Developments in the Field of Thermal Barrier Coatings, *J. Therm. Spray Technol.*, 2009, **18**(2), p 181-186
- [9] H. Dai, X. Zhong, J. Li, Y. Zhang, J. Meng, X. Cao, Thermal Stability of Double-Ceramic-Layer Thermal Barrier Coatings with various Coating Thickness, *Mater. Sci. Eng. A - Struct.*, 2006, **433**(1), p1-7
- [10] V. Viswanathan, G. Dwivedi, S. Sampath, Multimaterial Thermal Barrier Coating Systems: Design, Synthesis, and Performance Assessment, *J. Am. Ceram. Soc.*, 2015, **98**(6), p 1769-1777

- [11] M. Saremi, Z. Valefi, Thermal and Mechanical Properties of Nano-YSZ-Alumina Functionally Graded Coatings Deposited by Nano-Agglomerated Powder Plasma Spraying, *Ceram. Int.*, 2014, **40**(8), p 13453-13459
- [12] A. Portinham V., Teixeira, J. Carneiro, J. Martins, M.F. Costa, R. Vassen, D. Stoeber, Characterization of Thermal Barrier Coatings with a Gradient Porosity, *Surf. Coat. Technol.*, 2005, **195**(2), p 245-251
- [13] P. Carpio, E. Bannier, M.D. Salvador, R. Benavente, E. Sánchez, Multilayer and Particle Size-Graded YSZ Coatings Obtained by Plasma Spraying of Microand Nanostructured Feedstocks, *J. Therm. Spray Technol.*, 2014, **23**(8), p 1362-1372
- [14] S. Nath, I. Manna, J.D. Majumdar, Nanomechanical Behavior of Yttria Stabilized Zirconia (YSZ) Based Thermal Barrier Coating, *Ceram. Int.*, 2015, **41**(4), p 5247-5256
- [15] P. Carpio, E. Rayón, L. Pawlowski, A. Cattini, R. Benavente, E. Bannier, M.D. Salvador, E. Sánchez, Microstructure and Indentation Mechanical Properties of YSZ Nanostructured Coatings Obtained by Suspension Plasma Spraying, *Surf. Coat. Technol.*, 2013, **220**, p 237-243
- [16] H.B. Guo, H. Murakami, S. Kuroda, Effect of Hollow Spherical Powder Size Distribution on Porosity and Segmentation Cracks in Thermal Barrier Coatings, *J. Am. Ceram. Soc.*, 2006, **89**(12), p 3797-3804
- [17] R.S. Lima, A. Kucuk, C.C. Berndt, Integrity of Nanostructured Partially Stabilized Zirconia After Plasma Spray Processing, *Mater. Sci. Eng. A*, 2001, **313**(1), p 75–82

- [18] E. Rayón, V. Bonache, M.D. Salvador, E. Sánchez, Hardness and Young's Modulus Distributions in Atmospheric Plasma Sprayed WC-Co Coatings Using Nanoindentation, *Surf. Coat. Technol.*, 2011, **205**(17), p 4192-4197
- [19] J.A. Wollmershauser, B.N. Feigelson, E.P. Gorzkowski, C.T. Ellis, R. Goswami, S.B. Qadri, J.G. Tischler, F.J. Kub, R.K. Everett, An Extend Hardness Limit in Bulk Nanoceramics, *Acta Mater.*, 2014, **69**, p 9-16
- [20] L. Wang, Y. Wang, X.G. Sun, J.Q. He, Z.Y. Pan, C.H. Wang, Microstructure and Indentation Mechanical Properties of Plasma Sprayed Nano-Bimodal and Conventional ZrO<sub>2</sub>-8wt% Y<sub>2</sub>O<sub>3</sub> Thermal Barrier Coatings, *Vacuum*, 2012, **86**(8), p 1174-1185
- [21] G.S. Barroso, W. Krenkel, G. Motz, Low Thermal Conductivity Coating System for Application up to 1000 °C by Simple PDC Processing with Active and Passive Fillers, *J. Eur. Ceram. Soc.*, 2015, **35**(12), p.3339-3348
- [22] R. Ghasemi, R. Shoja-Razavi, R. Mozafarinia, H. Jamali, M. Hajizadh-Oghaz, R. Ahmadi-Pidani, The Influence of Laser Treatment on Hot Corrosion Behavior of Plasma-Sprayed Nanostructured Ytria Stabilized Zirconia Thermal Barrier Coatings, *J. Eur. Ceram. Soc.*, 2014, **34**(8) p 2013-2021
- [23] E. Rayón, V. Bonache, M.D. Salvador, E. Bannier, E. Sánchez, A. Denoirjean, H. Ageorges, Nanoindentation Study of the Mechanical and Damage Behaviour of Suspension Plasma Sprayed TiO<sub>2</sub> Coatings, *Surf. Coat. Technol.*, 2012, **206**(10), p 2655-2660
- [24] J.J. Roa, E. Jiménez-Piqué, R. Martínez, G. Ramírez, J.M. Tarragó, R. Rodríguez, L. Llanes, Contact Damage and Fracture Micromechanisms of

Multilayered TiN/CrN Coatings at Micro- and Nano-length Scales, Thin Solid Films, 2014, **571**(2) p 308-315



## Figure captions

Figure 1. Flow diagram showing the deposition process to obtain the two types of composite coatings: double layer (coatings M1 and M2) and graded (coatings G1 and G2).

Figure 2. Images acquired by FE-SEM microscope on the cross-section view of the coating M1 a), M2 b), G1 c) and G2 d).

Figure 3. Hardness and elastic modulus curves results acquired from the nanoindentation arrays performed on the cross-section of the a) M1, b) M2, c) G1 and d) G2 composite coatings. Indentations were done with a Berkovich tip at a 400nm maximum depth.

Figure 4.- Optical microscope images of the peeled-off material captured after the adhesion tests. The upper images sequence corresponds to the peeled-off material glued beneath dollies, the bottom pictures show the coatings onto substrates. Samples are M1 a), M2 b), G1 c) and G2 d). The bar scale corresponds to 2 mm.

Figure 5.- Image captured by optical microscope of the cross-section view in the zone when material removal took place by adhesion test on the M1 and M2 coatings.

Figure 6. Groove tracks and penetration curves on M-type composite coatings: up) the layer obtained from the microstructured feedstock is on bond coat (coating M1); down) the layer obtained from the nano-structured feedstock is on bond coat (coating M2).

## Table list

Table 1. Adhesion strength obtained for each tested coating of composites Ms and Gs.

Adhesion strength (MPa)			
M1	M2	G1	G2
8.8±1.2	3.4±0.9	5.7±1.8	5.2±1.2

## Figure list

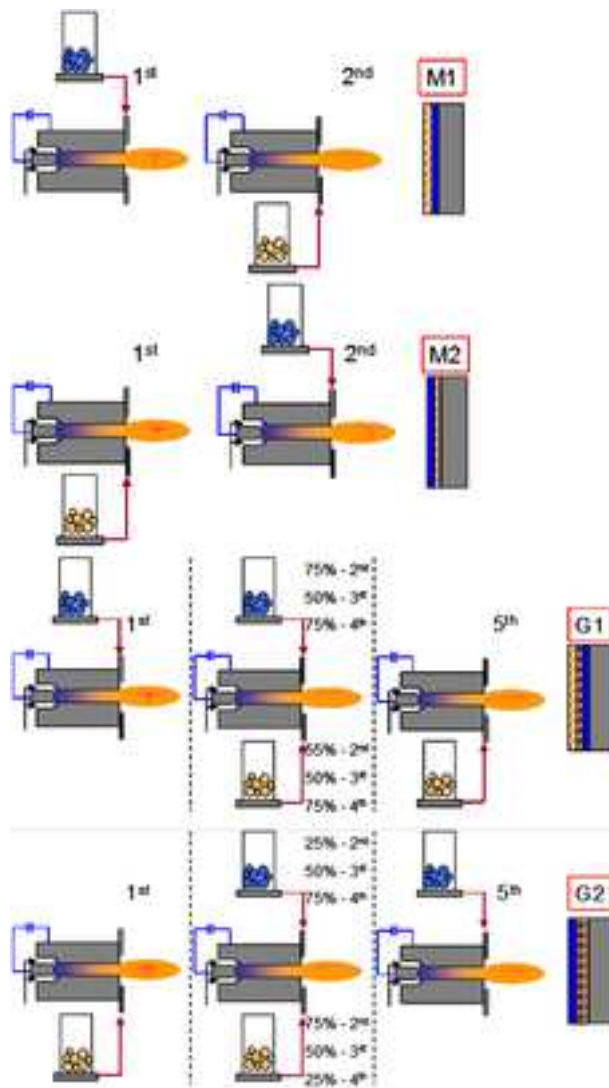


Figure 1

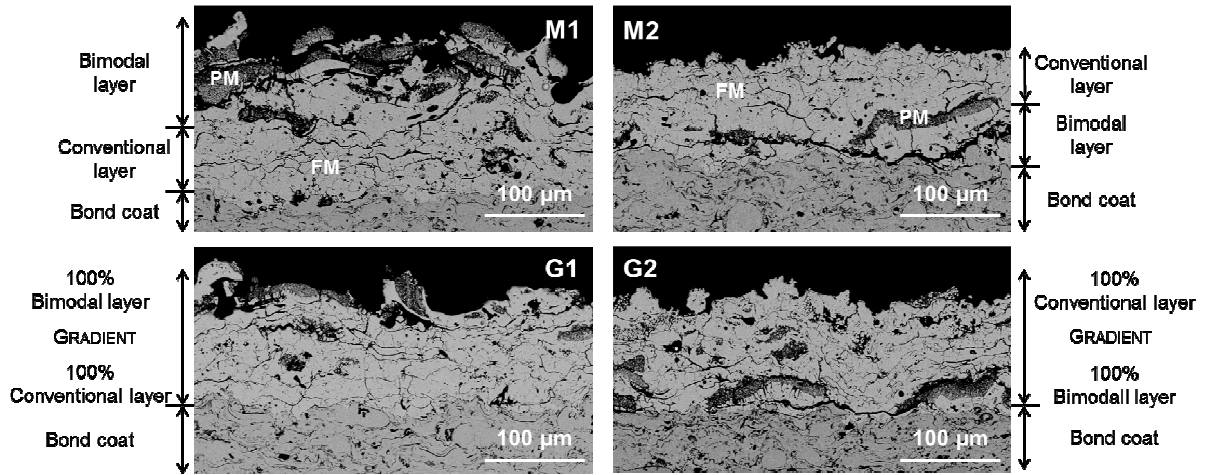


Figure 2

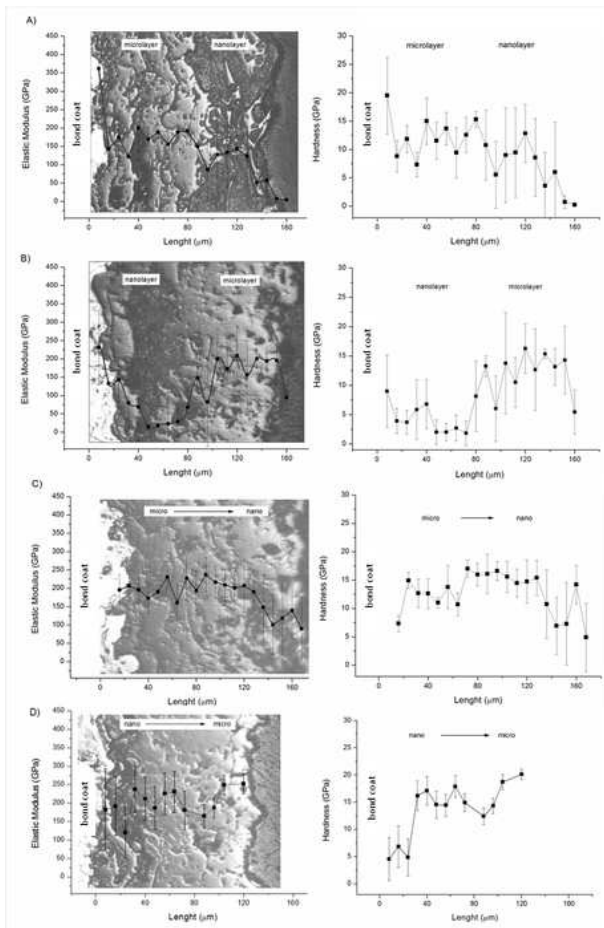


Figure 3

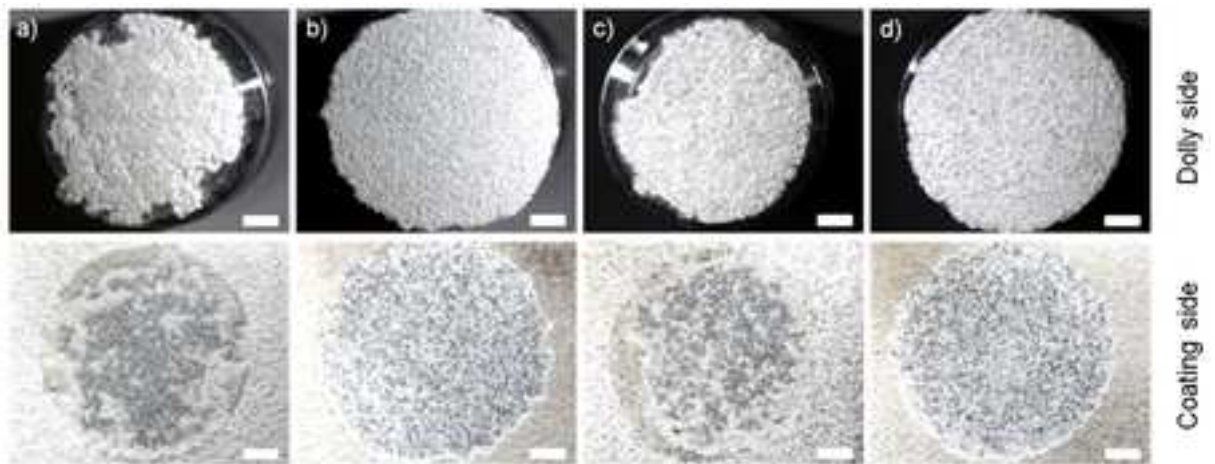


Figure 4

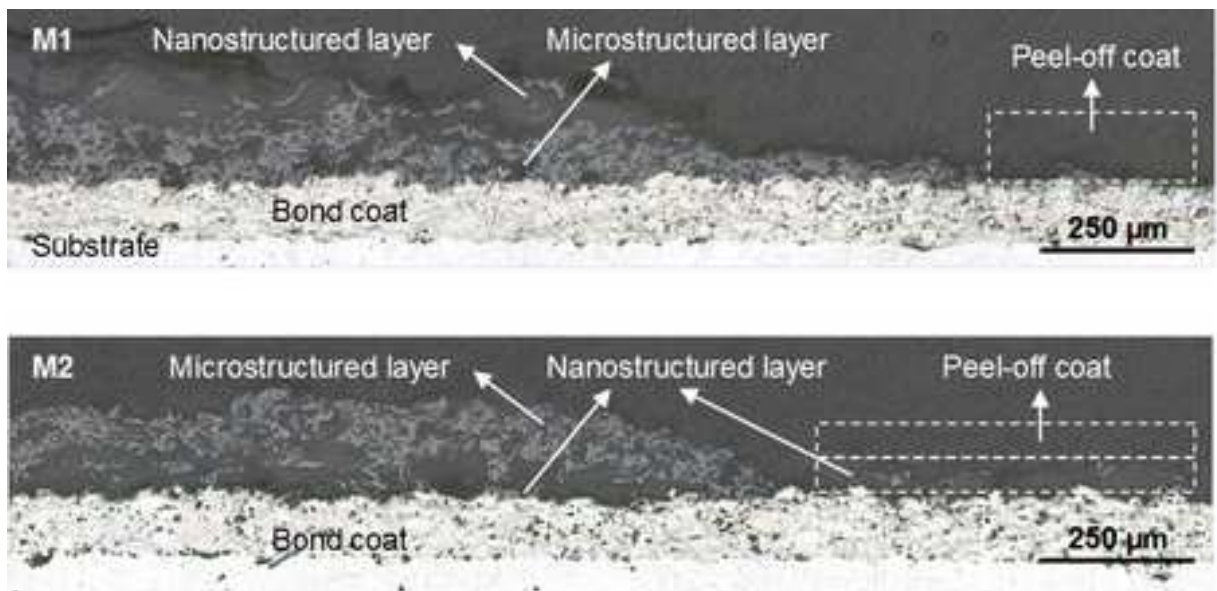


Figure 5

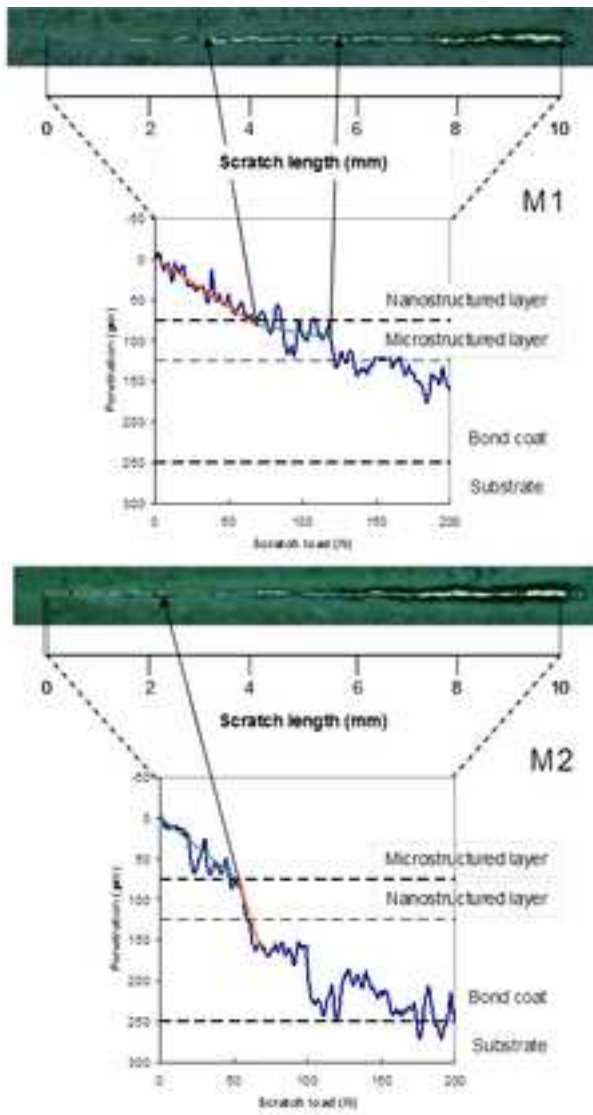


Figure 6